frontiers | Frontiers in Earth Science

TYPE Original Research
PUBLISHED 20 September 2022
DOI 10.3389/feart.2022.1016605

Analytical solution of mechanical response in cold region tunnels under transversely isotropic freeze–thaw circle induced by unidirectional freeze–thaw damage

Zhitao Lv, Mingchao Wu, Faming Huang* and Yi Cai

School of Infrastructure Engineering, Nanchang University, Nanchang, China

OPEN ACCESS

EDITED BY
Guang-Liang Feng,
Chinese Academy of Sciences (CAS),
China

REVIEWED BY
Guozhu Zhang,
Southeast University, China
Qiang Feng,
Shandong University of Science and
Technology, China

*CORRESPONDENCE
Faming Huang,
faminghuang@ncu.edu.cn

SPECIALTY SECTION
This article was submitted to
Geohazards and Georisks,
a section of the journal
Frontiers in Earth Science

RECEIVED 11 August 2022
ACCEPTED 25 August 2022
PUBLISHED 20 September 2022

CITATION
Lv Z, Wu M, Huang F and Cai Y (2022), Analytical solution of mechanical response in cold region tunnels under transversely isotropic freeze–thaw circle induced by unidirectional freeze–thaw damage.
Front. Earth Sci. 10:1016605.
doi: 10.3389/feart.2022.1016605

During the operation stage of cold region tunnels, the isotropic surrounding rock in a freeze–thaw circle suffers long-term unidirectional freeze–thaw cycles and gradually transforms into transversely isotropic material, which induces the variation of stress and displacement distribution of cold region tunnels. Aimed at this phenomenon, an analytical solution of mechanical response in cold region tunnels under transversely isotropic freeze–thaw circles induced by unidirectional freeze–thaw damage is proposed. The analytical solution is derived under two different states of the freeze–thaw circle: *1*) transversely isotropic and unfrozen state (state TU) and *2*) transversely isotropic and frozen state (state TF). In addition, the stress distribution in the lining and surrounding rock with a transversely isotropic freeze–thaw circle is analyzed. The transformation of the surrounding rock in a freeze–thaw circle from isotropic material into transversely isotropic material leads to the increase of stress in the lining, especially for a significant increase under state TF. Finally, the influence of the deterioration coefficient and the degree of anisotropy on the stress distribution in the lining is analyzed. The stress in the lining increases linearly as the deterioration coefficient decreases, while it increases nonlinearly as the degree of anisotropy decreases. The smaller the degree of anisotropy is, the greater the increase rate of the stress is. Moreover, the increase of stress with deterioration coefficient and degree of anisotropy under state TF is much greater than that under state TU. Both deterioration coefficient and degree of anisotropy decrease from 1.0 with increasing unidirectional freeze–thaw cycles suffered by surrounding rock, and, thus, induce the increase of stresses in the lining. In addition, the deterioration coefficient has a greater influence than the degree of anisotropy on the stress in the lining.

KEYWORDS

stress distribution, cold region tunnels, transversely isotropic freeze–thaw circle, mechanical response, unidirectional freeze–thaw

Introduction

With the economic growth and increasing traffic demand, more and more cold region tunnels are constructed in cold areas such as Alaska, north Japan, Russia, and Norway, especially in Tibet Plateau and north China. However, most cold region tunnels suffer destructive and troublesome frost damage induced by special climate and geological environment, which even leads to stability and safety problems (Huang et al., 2020, 2022).

The temperature field of cold region tunnels varies significantly above and below the freezing point every year due to the peculiar climate of tunnel sites (Li et al., 2015; Yu et al., 2018), resulting in the freezing and thawing of surrounding rock and groundwater, and, thus, induces various kinds of frost damages. As the temperature field is a basis for frost resisting, plenty of model experiments were performed to investigate the temperature evolution of cold region tunnels and the influence of factors such as airflow temperature (Zeng et al., 2017), inlet wind velocity (Liu L. et al., 2018), and construction disturbance (Zhang et al., 2018). Moreover, numerical models coupled the heat convection and heat conduction between airflow and surrounding rock were proposed to forecast the temperature evolution of cold region tunnels (Lai et al., 2005; Tan et al., 2014). Numerical models involving the influence of train-induced ventilation on temperature evolution were also established (Zhou et al., 2016).

Freeze proofing is a type of measure to resist frost damage, and the thermal insulation layer has currently been the most popular and effective method in freeze proofing. An optimization method to design a thermal insulation layer has been found by Li et al. (2017) based on a coupled heat-water numerical model. Feng et al. (2016) conducted physical modelling experiments in the Yuximolegai tunnel and investigated the reliability of the thermal insulation layer design. Li et al. (2020) analyzed the capacity degradation of thermal insulation materials after moisture absorption and complete freezing in cold region tunnels. There are also applications of other freeze-proofing methods, such as the ground heat exchanger system utilizing heat in deeper surrounding rock (Zhang et al., 2016, 2017; Chang et al., 2022).

Furthermore, the stress distribution and stability of cold region tunnels are significantly influenced by the temperature evolution and freezing of surrounding rock and groundwater. At present, stability analysis on cold region tunnels is mostly based on the freeze–thaw circle frost heave model first proposed by Lai et al. (2000). This model holds that frost heaving force is induced by the frost heave of the freeze–thaw circle, and solutions based on this model can be categorized into three kinds according to their assumptions. The first kind assumes the frost heave displacement mode of the freeze–thaw circle. For example, Gao et al. (2012) derived a solution assuming that displacement does not occur at the center line of the freeze–thaw circle when frost heave generates. The second kind of solution assumes isotropic frost heave in the freeze–thaw circle. According to this assumption, a visco-elastic stress solution (Lai et al., 2000) and an elasto-plastic stress solution (Feng et al., 2014) on cold region tunnels when the surrounding rock freezes have been developed. In addition, an elastic stress solution under non-axisymmetric stress has been derived by Feng et al. (2017), assuming isotropic frost heave in cold region tunnels. The third kind of solution assumes that the frost heave of the freeze–thaw circle is anisotropic. For example, Xia et al. (2018) proved the transversely isotropic frost heave of the freeze–thaw circle through frost heave experiments on rock and then established an elastic stress solution which considered this specific frost heaving property of surrounding rock in cold region tunnels. On the basis of the experimental study and elastic solution of Xia et al., Lv et al. (2019) further derived an elasto-plastic solution of stress with the same assumption of transversely isotropic frost heave in cold region tunnels and found a remarkable influence of transversely isotropic frost heave on stress distribution. Feng et al. (2019) established a similar elasto-plastic solution with a different yield criterion. Moreover, Liu W. et al. (2018) built an elasto-plastic solution of stress on cold region tunnels taking the coupling influence of anisotropic frost heaving property of surrounding rock, support strength, and support time into consideration.

However, most current stress solutions of cold region tunnels regard the mechanical properties of surrounding rock as invariant. In fact, surrounding rock suffers freeze–thaw cycles and deteriorates during the operation stage of cold region tunnels. Ding et al. (2020) investigated the deterioration in mechanical properties with freeze–thaw cycles in a tight sandstone and studied changes to its pore structure using nuclear magnetic resonance technology. Huang et al. (2022a, b) studied the pore structure change of red sandstone under freeze–thaw cycles by mercury intrusion porosimetry and found that both the uniaxial compressive strength and the triaxial compressive strength decrease due to the growth of macropores. Liu et al. (2020) investigated the effect of water saturation on the physico-mechanical properties of clay-bearing rock under freeze–thaw by testing the uniaxial compressive strength and P-wave velocity. Moreover, the damage model and damage constitutive model of rock to describe its deterioration under freeze–thaw action were built (Huang et al., 2021; Meng et al., 2021; Feng et al., 2022). Hence, the mechanical properties of rock in freeze–thaw circles evolve continuously as the suffered freeze–thaw cycles increase. Liu et al. (2019) developed a frost heaving force solution concerning the combined influence of decreasing elastic modulus and increasing void ratio of rock in a freeze–thaw circle resulting from the freeze–thaw action. In addition to the reducing mechanical parameters, experiments show that isotropic rocks transform into transversely isotropic materials under long-term unidirectional freeze–thaw action (Nakamura et al., 2009, 2012; Murton et al., 2016; Xia et al., 2018). When cold air in winter or hot air in summer flows into cold region tunnels, heat mainly transfers along the radial direction with the main temperature

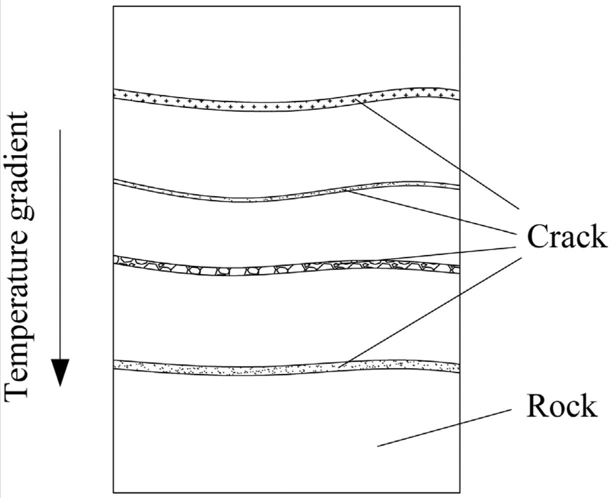

FIGURE 1
Crack distribution in rock induced by unidirectional freeze–thaw damage.

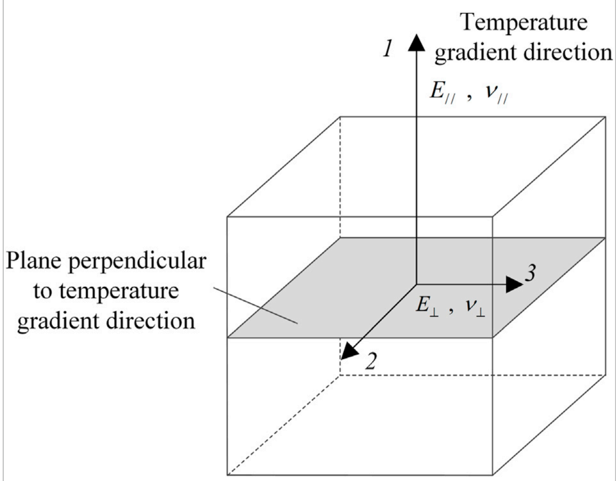

FIGURE 2
Transverse isotropy of rock induced by unidirectional freeze–thaw damage.

gradient in the radial direction, and the surrounding rock in the freeze–thaw circle suffers unidirectional freeze–thaw action. Consequently, the isotropic rock in the freeze–thaw circle gradually transforms into transversely isotropic material as the result of long-term unidirectional freeze–thaw action, and the aforementioned solutions are inapplicable for transversely isotropic surrounding rock.

Therefore, in this study, an analytical solution of the mechanical response of cold region tunnels with a transversely isotropic freeze–thaw circle induced by unidirectional freeze–thaw damage is established. The analytical solution is derived under two different states of the freeze–thaw circle: *1*) transversely isotropic and unfrozen state and *2*) transversely isotropic and frozen state. Furthermore, based on the solutions, the stress field in the lining and surrounding rock with a transversely isotropic freeze–thaw circle is analyzed, and the influence of the deterioration coefficient and the degree of anisotropy on the mechanical response of cold region tunnels is analyzed.

Mechanical model of cold region tunnels under a transversely isotropic freeze–thaw circle

Transversely isotropic freeze–thaw circle induced by unidirectional freeze–thaw damage

Lots of experiments show that layered cracks perpendicular to the temperature gradient direction will generate in a rock under long-term unidirectional freeze–thaw action (Nakamura et al., 2009, 2012; Murton et al., 2016; Xia et al., 2018), as shown in Figure 1. When the rock with layered cracks is considered a continuous medium, it is similar to the stratified rock in macro-mechanical properties and can be regarded as transversely isotropic material. As illustrated in Figure 2, any plane perpendicular to the temperature gradient direction is the plane of isotropy, and any line parallel to the temperature gradient direction is the axis of transverse isotropy. Therefore, isotropic rocks will gradually transform into transversely isotropic materials under unidirectional freeze–thaw conditions.

As illustrated in Figure 3, when the cold air in winter or the hot air in summer flows into cold region tunnels, heat mainly transfers along the radial direction with a prime temperature gradient in the radial direction, and the temperature gradient along the circumferential or axial direction is negligible (Lai et al., 2002; Zhang et al., 2002). Hence, the surrounding rock in freeze–thaw circles suffers unidirectional freeze–thaw action every year. Thus, the mechanical properties of rock in freeze–thaw circles gradually transform into transverse isotropy. As shown in Figure 4, the radial direction, namely, the temperature gradient direction, is the axis of transverse isotropy, and the cylindrical surface composed of the axial direction and circumferential direction, which is perpendicular to the radial direction, is the plane of isotropy.

Mechanical model of cold region tunnels

Figure 5 illustrates the mechanical model of the stress and deformation response of cold region tunnels with transversely isotropic rock in freeze–thaw circles induced by unidirectional

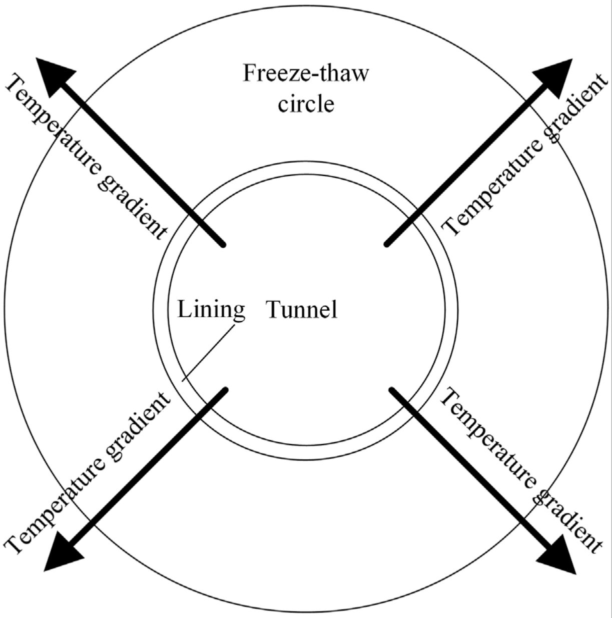

FIGURE 3
Temperature gradient in cold region tunnels.

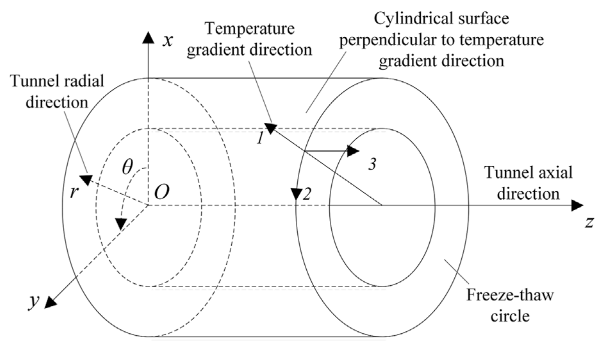

FIGURE 4
Transverse isotropy of freeze–thaw circle in cold region tunnels.

freeze–thaw damage. As displayed in Figure 5, in the initial state, when the construction of the tunnel completes, the surrounding rock is isotropic; after entering the cold season, the surrounding rock in the freeze–thaw circle freezes gradually, and, thus, the freeze–thaw circle is isotropic and frozen, which can be referred to as state F. During the operation of the tunnel, the surrounding rock in the freeze–thaw circle gradually transform into transversely isotropic material due to the unidirectional freeze–thaw damage. The stress and displacement in cold region tunnels will significantly change with the transformation of the freeze–thaw circle from isotropic material to transversely isotropic material. In the warm season, the freeze–thaw circle is transversely isotropic and unfrozen, which can be referred to as state TU; in the cold season, the freeze–thaw circle is transversely isotropic and frozen, which can be referred to as state TF, as shown in Figure 5. In Figure 5, zone I is the lining, and zone V is isotropic and unfrozen surrounding rock. Zone II is the isotropic and frozen surrounding rock in state F; zone III is the transversely isotropic and unfrozen surrounding rock in state TU; and zone IV is the transversely isotropic and frozen surrounding rock in state TF.

Moreover, in Figure 5, r_0 and r_1 represent the internal and external radius of lining, respectively; r_f represents the external radius of the freeze–thaw circle; R_0 extends somewhere far away. P_l is the radial stress act on the lining, and P_f represents the radial stress act on the interface between freeze–thaw circle and zone V. P_0 represent the initial ground stress.

The compressive stress, strain, and displacement are regarded as positive. To obtain the analytical solution of mechanical response under a transversely isotropic freeze–thaw circle, assumptions are introduced as follows:

(1) The cross-section of cold region tunnels is approximated as a circle.
(2) The plane strain condition is introduced.
(3) The surrounding rock and lining are considered as continuous, homogeneous, and elastic materials in each zone.
(4) The lining and the surrounding rock in zones II and V are isotropic material, whereas the surrounding rock in zones III and IV are transversely isotropic material induced by the unidirectional freeze–thaw damage.

Solution of mechanical response in cold region tunnels with a transversely isotropic freeze–thaw circle

Solution of mechanical response in cold region tunnels under state TU

Stress and displacement in a transversely isotropic and unfrozen freeze–thaw circle (zone III)

The constitutive relations of a transversely isotropic freeze–thaw circle in zone III can be written as (Lekhnitskii, 1981) follows:

$$\begin{cases} \varepsilon_r = a_{11}\sigma_r + a_{12}\sigma_\theta + a_{13}\sigma_z \\ \varepsilon_\theta = a_{12}\sigma_r + a_{22}\sigma_\theta + a_{23}\sigma_z \\ \varepsilon_z = a_{13}\sigma_r + a_{23}\sigma_\theta + a_{33}\sigma_z, \end{cases} \quad (1)$$

where ε and σ are the strain and stress, respectively; the subscript r, θ, and z refer to the radial, circumferential, and axial direction; $a_{11} = \frac{1}{E_r}$, $a_{12} = a_{13} = -\frac{\mu_{\theta r}}{E_r}$, $a_{22} = a_{33} = \frac{1}{E_\theta}$, and $a_{23} = -\frac{\mu_{\theta z}}{E_\theta}$; E_r is Young's modulus along the radial direction; E_θ is Young's

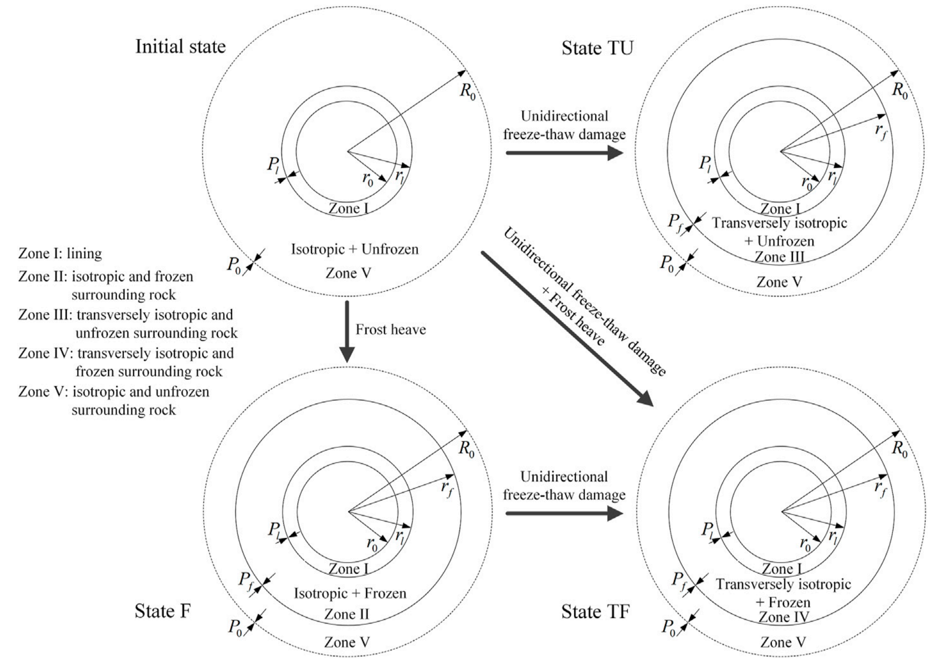

FIGURE 5
Mechanical model of cold region tunnels.

modulus in the isotropic cylindrical surface; $\mu_{\theta r}$ is the Poisson's ratio defining strain induced in the isotropic surface by stress applied in the radial direction; and $\mu_{\theta z}$ is the Poisson's ratio defining strain induced in the isotropic surface by stress applied in the surface.

Under the plane strain condition, $\varepsilon_z = 0$. Hence, σ_z can be acquired from Eq. 1:

$$\sigma_z = -\frac{1}{a_{33}}\left(a_{13}\sigma_r + a_{23}\sigma_\theta\right). \tag{2}$$

Substituting Eq. 2 into Eq. 1, ε_r and ε_θ can be obtained as follows:

$$\begin{cases} \varepsilon_r = \beta_{11}\sigma_r + \beta_{12}\sigma_\theta \\ \varepsilon_\theta = \beta_{12}\sigma_r + \beta_{22}\sigma_\theta, \end{cases} \tag{3}$$

where $\beta_{ij} = a_{ij} - \frac{a_{i3}}{a_{33}}a_{j3}$, (i, j= 1, 2).

According to the elasticity, the geometric equations and the compatibility condition of the axisymmetric problem are as follows:

$$\varepsilon_r = \frac{\mathrm{d}u_r}{\mathrm{d}r},\ \varepsilon_\theta = \frac{u_r}{r}, \tag{4a}$$

$$\varepsilon_r = \frac{d}{dr}\left(r\varepsilon_\theta\right), \tag{4b}$$

where u_r represents the displacement in the radial direction.

Moreover, the equilibrium equation of the axisymmetric problem is

$$r\frac{d\sigma_r}{dr} + \sigma_r - \sigma_\theta = 0. \tag{5}$$

Combining Eqs 3, 4b, and 5, the following equation can be acquired:

$$r^2\frac{d^2\sigma_r}{dr^2} + 3r\frac{d\sigma_r}{dr} - \left(\frac{\beta_{11}}{\beta_{22}} - 1\right)\sigma_r = 0. \tag{6}$$

The general solution of Eq. 6 is

$$\sigma_r = A_1 r^{n-1} + B_1 r^{-(n+1)}, \tag{7}$$

where A_1 and B_1 are undetermined integral constants, and $n = \sqrt{\frac{\beta_{11}}{\beta_{22}}}$.

The stress boundary conditions of zone III are:

$$\begin{cases} \sigma_r^{\mathrm{III}} = P_l\left(r = r_l\right) \\ \sigma_r^{\mathrm{III}} = P_f\left(r = r_f\right), \end{cases} \tag{8}$$

where the superscript III represents zone III. In addition, the following superscripts I, II, IV, and V represent zones I, II, IV, and V, respectively.

Considering Eqs 7 and 8, A_1 and B_1 can be obtained:

$$\begin{cases} A_1 = \dfrac{P_l r_l^{n+1} - P_f r_f^{n+1}}{r_l^{2n} - r_f^{2n}} \\ B_1 = \dfrac{P_f r_f^{n+1} r_l^{2n} - P_l r_l^{n+1} r_f^{2n}}{r_l^{2n} - r_f^{2n}}. \end{cases} \tag{9}$$

Combining Eqs 9, 7, and 5, σ_r and σ_θ in zone III can be acquired:

$$\begin{cases} \sigma_r^{\mathrm{III}} = \dfrac{P_l r_l^{n+1} - P_f r_f^{n+1}}{r_l^{2n} - r_f^{2n}} r^{n-1} + \dfrac{P_f r_f^{n+1} r_l^{2n} - P_l r_l^{n+1} r_f^{2n}}{r_l^{2n} - r_f^{2n}} r^{-(n+1)} \\ \sigma_\theta^{\mathrm{III}} = n \dfrac{P_l r_l^{n+1} - P_f r_f^{n+1}}{r_l^{2n} - r_f^{2n}} r^{n-1} - n \dfrac{P_f r_f^{n+1} r_l^{2n} - P_l r_l^{n+1} r_f^{2n}}{r_l^{2n} - r_f^{2n}} r^{-(n+1)}. \end{cases} \tag{10}$$

Plugging Eqs 1–3, ε_θ of zone III is acquired:

$$\begin{aligned} \varepsilon_\theta^{\mathrm{III}} = (\beta_{12} + n\beta_{22}) \frac{P_l r_l^{n+1} - P_f r_f^{n+1}}{r_l^{2n} - r_f^{2n}} r^{n-1} \\ + (\beta_{12} - n\beta_{22}) \frac{P_f r_f^{n+1} r_l^{2n} - P_l r_l^{n+1} r_f^{2n}}{r_l^{2n} - r_f^{2n}} r^{-(n+1)}. \end{aligned} \tag{11}$$

Plugging Eq. 11 to Eq. 4a, u_r of zone III is acquired:

$$\begin{aligned} u_r^{\mathrm{III}} = (\beta_{12} + n\beta_{22}) \frac{P_l r_l^{n+1} - P_f r_f^{n+1}}{r_l^{2n} - r_f^{2n}} r^{n} \\ + (\beta_{12} - n\beta_{22}) \frac{P_f r_f^{n+1} r_l^{2n} - P_l r_l^{n+1} r_f^{2n}}{r_l^{2n} - r_f^{2n}} r^{-n}. \end{aligned} \tag{12}$$

Stress and displacement in isotropic and unfrozen zone V and lining

According to the solution upon axisymmetric problem (Yu, 2000), the displacement and stress in isotropic and unfrozen zone V under the action of P_f at $r = r_f$ and P_0 at $r = R_0$ are as follows:

$$u_r^{\mathrm{V}} = \frac{1 + \mu_u}{E_u} \frac{r_f^2}{r} \left(P_0 - P_f\right), \tag{13}$$

$$\begin{cases} \sigma_r^{V} = P_0 \left(1 - \dfrac{r_f^2}{r^2}\right) + P_f \dfrac{r_f^2}{r^2} \\ \sigma_\theta^{V} = P_0 \left(1 - \dfrac{r_f^2}{r^2}\right) - P_f \dfrac{r_f^2}{r^2}, \end{cases} \tag{14}$$

where E_u and μ_u refer to Young's modulus and Poisson's ratio of the isotropic and unfrozen zone V, respectively.

In addition, according to the solution upon axisymmetric problem (Yu, 2000), the displacement and stress in lining (zone I) under the action of P_l at $r = r_l$ are as follows:

$$u_r^{\mathrm{I}} = \frac{1 + \mu_l}{E_l} \frac{(1 - 2\mu_l) r_l^2 r^2 + r_l^2 r_0^2}{r \left(r_l^2 - r_0^2\right)} P_l, \tag{15}$$

$$\begin{cases} \sigma_r^{\mathrm{I}} = \dfrac{r_l^2 \left(r^2 - r_0^2\right)}{\left(r_l^2 - r_0^2\right) r^2} P_l \\ \sigma_\theta^{\mathrm{I}} = \dfrac{r_l^2 \left(r_0^2 + r^2\right)}{\left(r_l^2 - r_0^2\right) r^2} P_l, \end{cases} \tag{16}$$

where E_l and μ_l refer to Young's modulus and Poisson's ratio of lining, respectively.

Continuity conditions and mechanical response solution

The continuity conditions of displacement at interfaces $r = r_l$ and $r = r_f$ are as follows:

$$u_r^{\mathrm{I}} = u_r^{\mathrm{III}} (r = r_l), \tag{17a}$$

$$u_r^{\mathrm{III}} = u_r^{\mathrm{V}} \left(r = r_f\right). \tag{17b}$$

The undetermined quantities are P_l and P_f, and they can be obtained by substituting Eqs 12, 13, and 15 to Eq. 17 as follows:

$$P_l = \frac{C_2 \frac{1+\mu_u}{E_u} P_0}{C_2 C_3 + \left[\beta_{12} - C_1 + \frac{1+\mu_u}{E_u}\right] \left[\beta_{12} + C_1 - \frac{1+\mu_l}{E_l} \frac{(1-2\mu_l) r_l^2 + r_0^2}{\left(r_l^2 - r_0^2\right)}\right]}, \tag{18a}$$

$$P_f = \frac{\frac{1+\mu_u}{E_u} P_0 \left[\beta_{12} + C_1 - \frac{1+\mu_l}{E_l} \frac{(1-2\mu_l) r_l^2 + r_0^2}{\left(r_l^2 - r_0^2\right)}\right]}{C_2 C_3 + \left[\beta_{12} - C_1 + \frac{1+\mu_u}{E_u}\right] \left[\beta_{12} + C_1 - \frac{1+\mu_l}{E_l} \frac{(1-2\mu_l) r_l^2 + r_0^2}{\left(r_l^2 - r_0^2\right)}\right]}, \tag{18b}$$

where $C_1 = \frac{n\beta_{22} \left(r_l^{2n} + r_f^{2n}\right)}{r_l^{2n} - r_f^{2n}}$, $C_2 = \frac{2n\beta_{22} r_f^{n+1} r_l^{n-1}}{r_l^{2n} - r_f^{2n}}$, and $C_3 = \frac{2n\beta_{22} r_l^{n+1} r_f^{n-1}}{r_l^{2n} - r_f^{2n}}$.

Finally, substituting the value of P_l and P_f into Eqs 15 and 16, the stress and displacement response in the lining under state TU can be acquired. Similarly, substituting P_l and P_f into Eqs 13 and 14, the stress and displacement response in the freeze–thaw circle under state TU can also be acquired.

Solution of the mechanical response in cold region tunnels under state TF

Stress and displacement in a transversely isotropic and frozen freeze–thaw circle (zone IV)

In the frozen zone IV, the total strain of surrounding rock consists of the strain resulting from local stress and the frost heaving strain. Therefore, the constitutive relations of the transversely isotropic and frozen rock in the freeze–thaw circle in zone IV are as follows:

$$\begin{cases} \varepsilon_r = a_{11}\sigma_r + a_{12}\sigma_\theta + a_{13}\sigma_z - \varepsilon_r^f \\ \varepsilon_\theta = a_{12}\sigma_r + a_{22}\sigma_\theta + a_{23}\sigma_z - \varepsilon_\theta^f \\ \varepsilon_z = a_{13}\sigma_r + a_{23}\sigma_\theta + a_{33}\sigma_z - \varepsilon_z^f, \end{cases} \tag{19}$$

where ε_r^f, ε_θ^f, and ε_z^f represent the frost heaving strains along the radial, circumferential, and axial directions, respectively; the meanings of the other symbols are the same as those in section 3.1, whereas the related parameters should take the values under the frozen state. Moreover, ε_r^f, ε_θ^f, and ε_z^f can be expressed by volumetric frost heaving strain $\varepsilon_{\mathrm{v}}^f$ (Xia et al., 2018; Lv et al., 2019):

$$\begin{cases} \varepsilon_r^f = \dfrac{k}{k+2} \varepsilon_{\mathrm{v}}^f \\ \varepsilon_\theta^f = \varepsilon_z^f = \dfrac{1}{k+2} \varepsilon_{\mathrm{v}}^f, \end{cases} \tag{20}$$

where ϵ_r^f, and k is the anisotropic frost heave coefficient defined as the ratio of ϵ_r^f to ϵ_θ^f.

Under the plane strain condition, $\varepsilon_z = 0$. Hence, σ_z can be acquired from Eq. 19:

$$\sigma_z = -\frac{1}{a_{33}}\left(a_{13}\sigma_r + a_{23}\sigma_\theta - \varepsilon_\theta^f\right). \tag{21}$$

Substituting Eq. 21 into Eq. 19, ε_r and ε_θ can be obtained:

$$\begin{cases} \varepsilon_r = \beta_{11}\sigma_r + \beta_{12}\sigma_\theta + \beta_1\varepsilon_\theta^f \\ \varepsilon_\theta = \beta_{12}\sigma_r + \beta_{22}\sigma_\theta + \beta_2\varepsilon_\theta^f, \end{cases} \tag{22}$$

where $\beta_{ij} = a_{ij} - \frac{a_{i3}}{a_{33}}a_{j3}$, (i, j= 1, 2); $\beta_1 = \frac{a_{13}}{a_{33}} - k$, and $\beta_2 = \frac{a_{23}}{a_{33}} - 1$.

Combining Eqs 22, 4b, and 5, the following equation can be acquired:

$$r^2\frac{d^2\sigma_r}{dr^2} + 3r\frac{d\sigma_r}{dr} - \left(\frac{\beta_{11}}{\beta_{22}} - 1\right)\sigma_r = \frac{\beta_1 - \beta_2}{\beta_{22}}\varepsilon_\theta^f. \tag{23}$$

The general solution of Eq. 23 can be obtained as follows:

$$\sigma_r = A_2 r^{n-1} + B_2 r^{-(n+1)} - \frac{\beta_1 - \beta_2}{\beta_{11} - \beta_{22}}\varepsilon_\theta^f, \tag{24}$$

where A_2 and B_2 are undetermined integral constants, and $n = \sqrt{\frac{\beta_{11}}{\beta_{22}}}$.

The stress boundary conditions of zone IV are

$$\begin{cases} \sigma_r^{\mathrm{IV}} = P_l\,(r = r_l) \\ \sigma_r^{\mathrm{IV}} = P_f\left(r = r_f\right). \end{cases} \tag{25}$$

Plugging Eq. 24 into Eq. 25, A_2 and B_2 are acquired:

$$\begin{cases} A_2 = \dfrac{P_l r_l^{n+1} - P_f r_f^{n+1} + \dfrac{\beta_1 - \beta_2}{\beta_{11} - \beta_{22}}\varepsilon_\theta^f\left(r_l^{n+1} - r_f^{n+1}\right)}{r_l^{2n} - r_f^{2n}} \\ B_2 = \dfrac{P_f r_f^{n+1} r_l^{2n} - P_l r_l^{n+1} r_f^{2n} + \dfrac{\beta_1 - \beta_2}{\beta_{11} - \beta_{22}}\varepsilon_\theta^f\left(r_l^{2n} r_f^{n+1} - r_l^{n+1} r_f^{2n}\right)}{r_l^{2n} - r_f^{2n}} \end{cases}. \tag{26}$$

Combining Eqs 26, 24, and 5, σ_θ in zone IV can be obtained:

$$\sigma_\theta^{\mathrm{IV}} = nA_2 r^{n-1} - nB_2 r^{-(n+1)} - \frac{\beta_1 - \beta_2}{\beta_{11} - \beta_{22}}\varepsilon_\theta^f. \tag{27}$$

Substituting Eqs 27 and 24 into Eq. 22, ε_θ in zone IV can be obtained. Then, substituting ε_θ into Eq. 4a, u_r in zone IV can be obtained:

$$u_r^{\mathrm{IV}} = \left(\beta_{12} + n\beta_{22}\right)A_2 r^n + \left(\beta_{12} - n\beta_{22}\right)B_2 r^{-n} - \frac{\beta_1 - \beta_2}{\beta_{11} - \beta_{22}}\varepsilon_\theta^f\left(\beta_{12} + \beta_{22}\right)r + \beta_2\varepsilon_\theta^f r. \tag{28}$$

Continuity conditions and mechanical response solution

The continuity conditions of displacement at interfaces $r = r_1$, $r = r_f$ are as follows:

$$u_r^{\mathrm{I}} = u_r^{\mathrm{IV}}\,(r = r_l), \tag{29a}$$

$$u_r^{\mathrm{IV}} = u_r^{\mathrm{V}}\left(r = r_f\right), \tag{29b}$$

The stress and displacement in isotropic and unfrozen zone V and lining (zone I) under state TF are the same as those given in Eqs 13–16, except that P_l and P_f should take the values under state TF. The undetermined quantities are P_l and P_f, and they can be obtained through plugging Eqs 13, 15, and 28 into Eq. 29:

$$P_l = \frac{\frac{1+\mu_u}{E_u}C_2P_0 - \frac{\beta_1-\beta_2}{\beta_{11}-\beta_{22}}\varepsilon_\theta^f\left[\left(C_1 - C_2 - \beta_{22}\right)\left(\beta_{12} - C_1 + \frac{1+\mu_u}{E_u}\right) + C_2\left(C_3 - C_1 - \beta_{22}\right)\right] - \beta_2\varepsilon_\theta^f\left[C_2 + \left(\beta_{12} - C_1 + \frac{1+\mu_u}{E_u}\right)\right]}{\left[C_2C_3 + \left(\beta_{12} + C_1 - \frac{1+\mu_l}{E_l}\frac{\left(1-2\mu_l\right)r_l^2 + r_0^2}{\left(r_l^2 - r_0^2\right)}\right)\left(\beta_{12} - C_1 + \frac{1+\mu_u}{E_u}\right)\right]}, \tag{30a}$$

$$P_f = \frac{\left(\beta_{12} + C_1 - \frac{1+\mu_l}{E_l}\frac{\left(1-2\mu_l\right)r_l^2 + r_0^2}{\left(r_l^2 - r_0^2\right)}\right)}{C_2}P_l + \frac{\frac{\beta_1-\beta_2}{\beta_{11}-\beta_{22}}\varepsilon_\theta^f\left(C_1 - C_2 - \beta_{22}\right) + \beta_2\varepsilon_\theta^f}{C_2}, \tag{30b}$$

where C_1, C_2, and C_3 are the same as those in section 3.1 except that the related parameters should take the values under the frozen state.

Finally, substituting the value of P_l and P_f into the corresponding formulas, the stress and displacement in the lining and freeze–thaw circle under state TF can be acquired.

Solution of stress and displacement in cold region tunnels under initial state and state F

To analyze the effect of transversely isotropic rock in freeze–thaw circles on the mechanical response of cold region tunnels, comparisons among the initial state, state F, state TU, and state TF are necessary. Hence, the solutions of stress and displacement in cold region tunnels under initial state and state F are also provided here.

The stress and displacement in the lining (zone I) under the initial state are the same as those given in Eqs 15 and 16, except that P_l should take the value under the initial state. In addition, according to the solution to the axisymmetric problem (Yu, 2000), the radial displacement and stress in isotropic and unfrozen zone V under the action of P_l at $r = r_l$ and P_0 at $r = R_0$ are acquired:

$$u_r^{\mathrm{V}} = \frac{1+\mu_u}{E_u}\frac{r_l^2}{r}\left(P_0 - P_l\right), \tag{31}$$

TABLE 1 Parameters of the section K105+785 in the cold region tunnel.

Parameter	r_0(m)	r_l(m)	r_f(m)	E_l(MPa)	μ_l	P_0(MPa)
Value	4.55	5.45	6.85	28,300	0.18	3.0
Parameter	E_u(MPa)	μ_u	E_f(MPa)	μ_f	ϵ_V^f	k
Value	25,000	0.37	27,500	0.37	0.45%	1.5

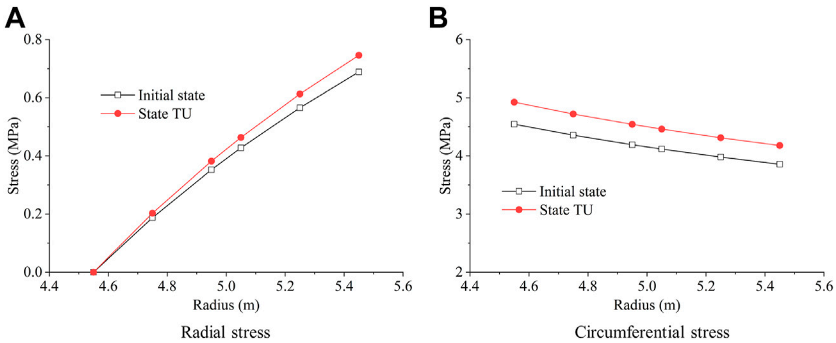

FIGURE 6
Stress of lining under initial state and state TU.

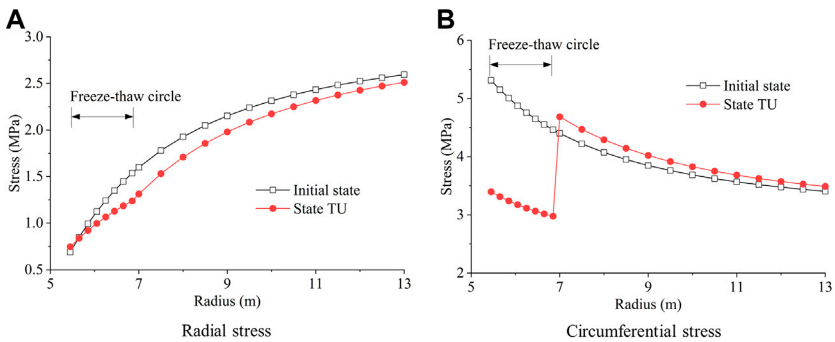

FIGURE 7
Stress of surrounding rock under initial state and state TU.

$$\begin{cases} \sigma_r^{\mathrm{V}} = P_0\left(1 - \dfrac{r_1^2}{r^2}\right) + P_l\dfrac{r_l^2}{r^2} \\ \sigma_\theta^{\mathrm{V}} = P_0\left(1 + \dfrac{r_l^2}{r^2}\right) - P_l\dfrac{r_l^2}{r^2} \end{cases}. \tag{32}$$

The displacement continuity conditions at interface $r = r_l$ is

$$u_r^{\mathrm{I}} = u_r^{\mathrm{V}}(r = r_l). \tag{33}$$

The undetermined quantity is P_l, and it is obtained through plugging Eqs 15 and 31 into Eq. 33 as follows:

$$P_l = \frac{\frac{1+\mu_u}{E_u}P_0}{\frac{1+\mu_l}{E_l}\frac{(1-2\mu_l)r_l^2+r_0^2}{r_l^2-r_0^2} + \frac{1+\mu_u}{E_u}}, \tag{34}$$

Finally, substituting the value of P_l into the corresponding formulas, the stress and displacement of lining and surrounding rock under the initial state can be acquired.

Furthermore, the stress and displacement of isotropic and unfrozen zone V and lining (zone I) under state F are the same as those given in Eqs 13–16, except that P_l and P_f should take the values under state F. The solutions of P_l and P_f under state F

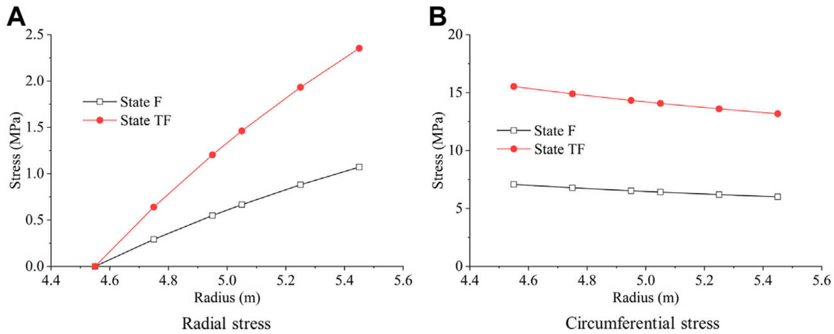

FIGURE 8
Stress of lining under state F and state TF.

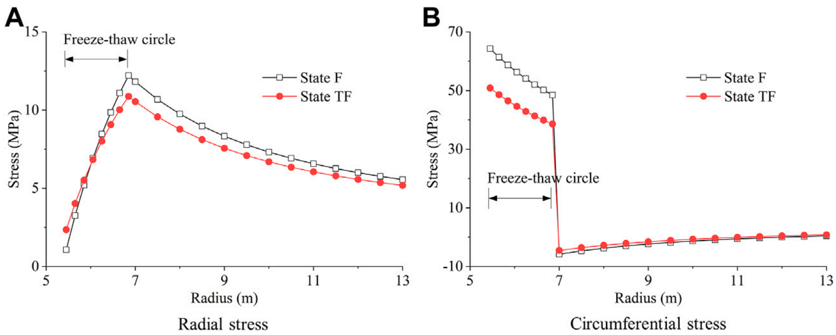

FIGURE 9
Stress of surrounding rock under state F and state TF.

have been proposed by Lv et al. (2019), namely, Eq. 38 or Eq. 39 in the study by Lv et al. (2019). In addition, the solutions of stress and displacement in the isotropic and frozen zone II under state F have also been proposed by Lv et al. (2019), namely, Eqs 34 and 35 in the study by Lv et al. (2019).

Case study

Stress distribution in the lining and surrounding rock

The proposed analytical solutions of stress and displacement under states TU and TF are extensions of the stress analysis on cold region tunnels involving transversely isotropic rock in freeze–thaw circle induced by unidirectional freeze–thaw damage. The engineering case in the study by Lv et al. (2019) can be referred to analyze the effect of a transversely isotropic freeze–thaw circles on the mechanical response of cold region tunnels. The related parameters are presented in Table 1, and E_f and μ_f in Table 1 are Young's modulus and Poisson's ratio of the isotropic and frozen surrounding rock (zone II).

During the operation stage of the cold region tunnel, the surrounding rock in the freeze–thaw circle gradually transforms to the transversely isotropic material resulting from unidirectional freeze–thaw damage, and E_r and E_θ also gradually decreases as the deterioration. To describe the deterioration effect of freeze–thaw damage on surrounding rock, the deterioration coefficient k_d is defined as E_θ/E_u under state TU or E_θ/E_f under state TF. Moreover, the degree of anisotropy k_a is defined as E_r/E_θ to describe the evolution of the transverse isotropy. Both k_d and k_a decrease from 1.0 with the increasing freeze–thaw cycles. In addition, the variation of Poisson's ratio is not considered.

Under the initial state, the radial stress act on the lining P_l calculated by the solution under the initial state is 0.69 MPa. Furthermore, under state TU, if $E_r = E_\theta = E_u$ and $\mu_{\theta r} = \mu_{\theta z} = \mu_u$ are assumed, namely, $k_d = 1.0$ and $k_a = 1.0$, state TU transforms to the initial state. In this special case, P_l calculated by the

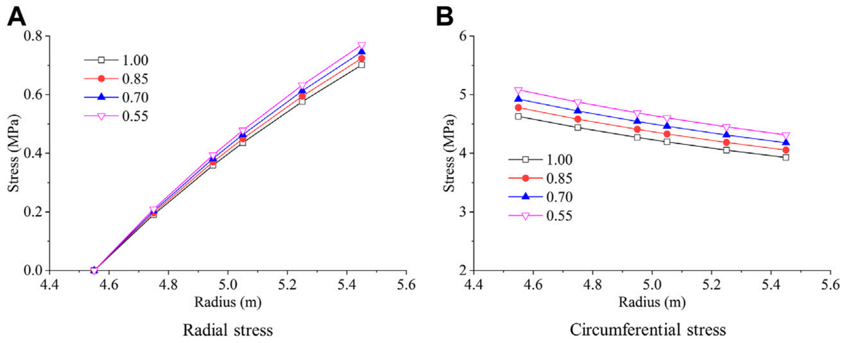

FIGURE 10
Influence of deterioration coefficient k_d under state TU.

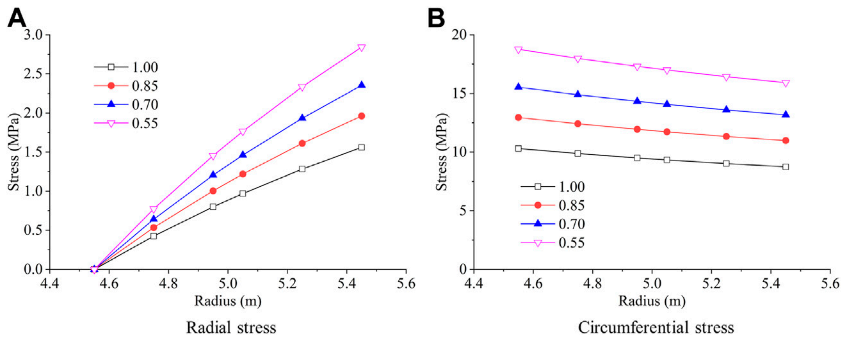

FIGURE 11
Influence of deterioration coefficient k_d under state TF.

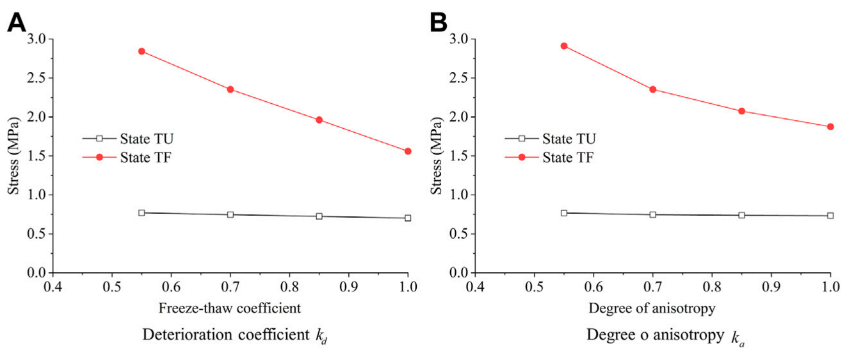

FIGURE 12
Influence of deterioration coefficient k_d and degree of anisotropy k_a on P_l.

solution under state TU is 0.69 MPa. The special case that $E_r = E_\theta = E_u$ and $\mu_{\theta r} = \mu_{\theta z} = \mu_u$ under state TU is identical to the initial state, and the results of P_l calculated by the two abovementioned different solutions are the same, thus, the correctness of the derivation processes of the solution under state TU can be verified.

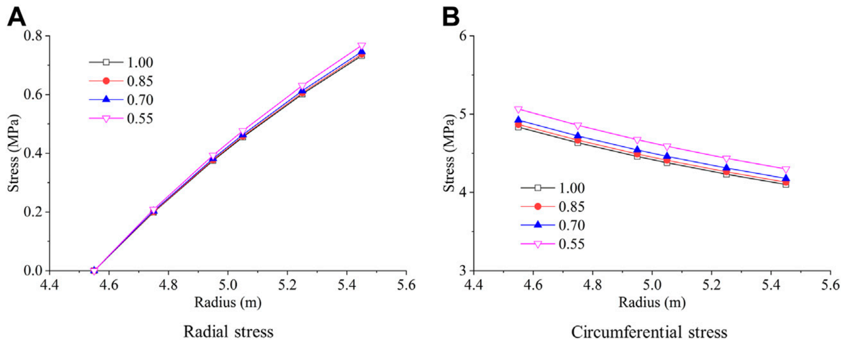

FIGURE 13
Influence of degree of anisotropy k_a under state TU.

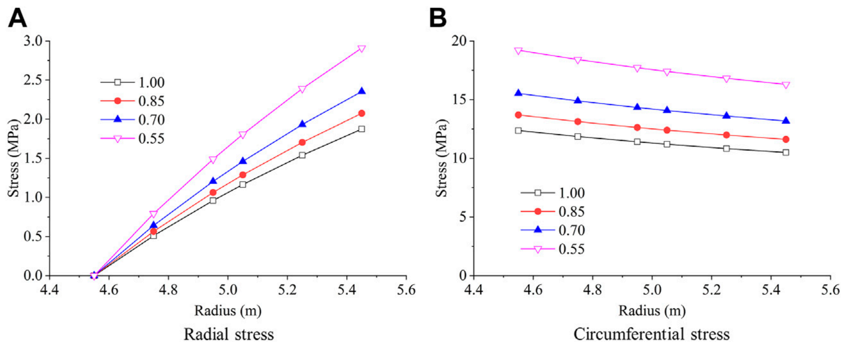

FIGURE 14
Influence of degree of anisotropy k_a under state TF.

Under state F, P_l calculated by the solution under state F is 1.07 MPa. Moreover, under state TF, if $E_r = E_\theta = E_f$ and $\mu_{\theta r} = \mu_{\theta z} = \mu_f$ are assumed, namely, $k_d = 1.0$ and $k_a = 1.0$, state TF transforms to state F. In this special case, P_l calculated by the solution under state TF is 1.08 MPa. The special case that $E_r = E_\theta = E_f$ and $\mu_{\theta r} = \mu_{\theta z} = \mu_f$ under state TF is identical to state F, and the results of P_l calculated by the solutions under state F and state TF are the same, which verifies the correctness of the derivation processes of the solution under state TF.

To study the mechanical response of cold region tunnels under a transversely isotropic freeze–thaw circle, the stress distribution in lining and surrounding rock in the case that $k_d = 0.7$ and $k_a = 0.7$ under states TU and TF are shown in Figures 6–9. Under state TF, $E_\theta = k_d E_f$, $E_r = k_a E_\theta$, and $\mu_{\theta r} = \mu_{\theta z} = \mu_f$. The other parameters are included in Table 1. To demonstrate the influence of the transverse isotropy of the freeze–thaw circle, the stress distribution under the initial state and state F are also exhibited in Figures 6–9.

The surrounding rock is unfrozen under the initial state and state TU. The stress distribution in the lining is similar under these two states, whereas the radial and circumferential stress in the lining increase by about 8% when the surrounding rock in the freeze–thaw circle transforms from isotropic material into transversely isotropic material, as displayed in Figure 6. In addition, the radial stress in surrounding rock under state TU is gently less than that under the initial state, and the greatest difference occurs at the outer interface of the freeze–thaw circle, as displayed in Figure 7. Phenomenon of discontinuity generates in the circumferential stress of surrounding rock under state TU, and the circumferential stress in the freeze–thaw circle under state TU is significantly less than that under the initial state.

The surrounding rock in the freeze–thaw circle is frozen under states F and TF. The stress in the lining under state TF significantly increases to be greater than two times of that under state F when the surrounding rock in the freeze–thaw circle transforms from isotropic material into transversely isotropic material, as illustrated in Figure 8. For example, the radial stress at the outer interface of the lining is 1.07 MPa under state F, while it increases to 2.35 MPa under state TF. Moreover, the difference of radial stress in surrounding rock under states F and TF is slight, and the circumferential stress in the freeze–thaw circle under state TF is less than that under state F, as illustrated in Figure 9.

Therefore, the transformation of surrounding rock in the freeze–thaw circle from isotropic material into transversely isotropic material adversely affects the stress distribution in the lining, especially for state TF, under which the stress in the lining increases significantly. Hence, the influence of the transversely isotropic freeze–thaw circle should be considered to maintain the long-term stability of cold region tunnels.

Analysis of influencing factors

The abovementioned engineering case can be considered to research the effect of the deterioration coefficient k_d and the degree of anisotropy k_a on the mechanical response of cold region tunnels. In the base condition, values of k_d = 0.7 and k_a = 0.7 are taken, and values of other parameters are listed in Table 1. Change the value of k_d or k_a in the base condition to study their influences.

Figures 10 and 11 show the influence of the deterioration coefficient k_d on the stress in the lining under states TU and TF, respectively. The stress in the lining increases uniformly for both states TU and TF as the decrease of k_d, whereas the increase of stress under state TF is much greater. For example, as k_d decreases from 1.0 to 0.55, the radial stress at outer interface of the lining increases by 10% under state TU, while it increases by 80% under state TF.

Moreover, Figure 12 shows the variation of the pressure act on the lining P_l with k_d and k_a. As k_d decreases from 1.0 to 0.55, P_l linearly increases from 1.56 to 2.84 MPa under state TF and it increases from 0.70 to 0.77 MPa under state TU. k_d has greater influence on P_l under state TF. k_d decreases from 1.0 as unidirectional freeze–thaw cycles suffered by surrounding rock increases, and, thus, induces the increase of the radial and circumferential stresses in the lining. Furthermore, k_a has much greater influence on P_l under state TF than that under state TU. As k_a decreases from 1.0 to 0.55, the radial stress at outer interface of the lining increases by 5% under state TU, while it increases by 55% under state TF. k_a decreases from 1.0 as unidirectional freeze–thaw cycles suffered by surrounding rock increases, and thus induces the increase of the radial and circumferential stresses in the lining.

Figures 13 and 14 show the influence of the degree of anisotropy k_a on the stress in the lining under states TU and TF, respectively. The stress in the lining increases nonlinearly for both states TU and TF as the decrease of k_a. The smaller the k_a is, the greater the increase rate of the stress is. For example, under state TF, the circumferential stress at inner surface of the lining increases from 10.50 to 11.62 MPa, as k_a decreases from 1.0 to 0.85, whereas it increases from 13.18 to 16.30 MPa, as k_a decreases from 0.70 to 0.55. Moreover, the increase of stress with k_a under state TF is much greater that under state TU. Comparing Figures 10–12 with Figures 13 and 14, k_d has greater influence than k_a on the stress in the lining.

Conclusion

In cold region tunnels, surrounding rock in a freeze–thaw circle suffers unidirectional freeze–thaw cycles during the operation process, and, thus, isotropic surrounding rocks gradually transform into transversely isotropic materials. Based on this phenomenon, an analytical solution to the mechanical response of cold region tunnels with a transversely isotropic freeze–thaw circle induced by unidirectional freeze–thaw damage is proposed. The analytical solution is derived under two different states of the freeze–thaw circle: *1*) transversely isotropic and unfrozen state and *2*) transversely isotropic and frozen state.

Additionally, the stress distribution in the lining and surrounding rock with a transversely isotropic freeze–thaw circle is analyzed. The transformation of the surrounding rock in a freeze–thaw circle from isotropic material into transversely isotropic material adversely affects the stress distribution in the lining, especially in the transversely isotropic and frozen state, under which the stress in the lining increases significantly.

Finally, the influence of the deterioration coefficient k_d and the degree of anisotropy k_a on the mechanical response in cold region tunnels is analyzed. The stress in the lining increases linearly with the decrease of k_d, whereas the increase of stress under the transversely isotropic and frozen state is much greater. The stress in the lining increases nonlinearly with the decrease of k_a. The smaller the k_a is, the greater the increase rate of the stress is. Moreover, the increase of stress with k_a under the transversely isotropic and frozen state is much greater than that under the transversely isotropic and unfrozen state. Both k_d and k_a decrease from 1.0 as unidirectional freeze–thaw cycles suffered by surrounding rock increase, and, thus, induce the increase of stresses in the lining. In addition, k_d has a greater influence than k_a on the stress in the lining.

Data availability statement

The raw data supporting the conclusions of this article will be made available by the authors, without undue reservation.

Author contributions

ZL: funding acquisition, writing—original draft, and methodology. MW: data curation and validation. FH: conceptualization, writing—review and editing. YC: formal analysis and investigation.

Funding

This research was supported by the National Natural Science Foundation of China (No. 52108370) and Jiangxi Provincial Natural Science Foundation (No. 20212BAB214062).

Conflict of interest

The authors declare that the research was conducted in the absence of any commercial or financial relationships that could be construed as a potential conflict of interest.

Publisher's note

All claims expressed in this article are solely those of the authors and do not necessarily represent those of their affiliated organizations, or those of the publisher, the editors, and the reviewers. Any product that may be evaluated in this article, or claim that may be made by its manufacturer, is not guaranteed or endorsed by the publisher.

References

Chang, Z., Catani, F., Huang, F., Liu, G., Meena, S., Huang, J., et al. (2022). Landslide susceptibility prediction using slope unit-based machine learning models considering the heterogeneity of conditioning factors. *J. Rock Mech. Geotechnical Eng.* doi:10.1016/j.jrmge.2022.07.009

Ding, S., Jia, H., Zi, F., Dong, Y., and Yao, Y. (2020). Frost damage in tight sandstone: Experimental evaluation and interpretation of damage mechanisms. *Materials* 13, 4617. doi:10.3390/ma13204617

Feng, Q., Fu, S., Wang, C., Liu, W., Wang, Y., and Qiao, W. (2019). Analytical elasto-plastic solution for frost force of cold-region tunnels considering anisotropic frost heave in the surrounding rock. *KSCE J. Civ. Eng.* 23, 3831–3842. doi:10.1007/s12205-019-1446-7

Feng, Q., Jiang, B.-S., Zhang, Q., and Wang, G. (2016). Reliability research on the 5-cm-thick insulation layer used in the Yuximolegai tunnel based on a physical model test. *Cold Regions Sci. Technol.* 124, 54–66. doi:10.1016/j.coldregions.2016.01.001

Feng, Q., Jiang, B.-S., Zhang, Q., and Wang, L. (2014). Analytical elasto-plastic solution for stress and deformation of surrounding rock in cold region tunnels. *Cold Regions Sci. Technol.* 108, 59–68. doi:10.1016/j.coldregions.2014.08.001

Feng, Q., Jin, J., Zhang, S., Liu, W., Yang, X., and Li, W. (2022). Study on a damage model and uniaxial compression simulation method of frozen-thawed rock. *Rock Mech. Rock Eng.* 55, 187–211. doi:10.1007/s00603-021-02645-2

Feng, Q., Liu, W., and Jiang, B.-S. (2017). Analytical solution for the stress and deformation of rock surrounding a cold-regional tunnel under unequal compression. *Cold Regions Sci. Technol.* 139, 1–10. doi:10.1016/j.coldregions.2017.04.003

Gao, G. Y., Chen, Q. S., Zhang, Q. S., and Chen, G. Q. (2012). Analytical elasto-plastic solution for stress and plastic zone of surrounding rock in cold region tunnels. *Cold Regions Sci. Technol.* 72, 50–57. doi:10.1016/j.coldregions.2011.11.007

Huang, F., Cao, Z., Jiang, S., Zhou, C., Huang, Z., and Guo, Z. (2020). Landslide susceptibility prediction based on a semi-supervised multiple-layer perceptron model. *Landslides* 17, 2919–2930. doi:10.1007/s10346-020-01473-9

Huang, F., Chen, J., Liu, W., Huang, J., Hong, H., and Chen, W. (2022). Regional rainfall-induced landslide hazard warning based on landslide susceptibility mapping and a critical rainfall threshold. *Geomorphology* 408, 108236. doi:10.1016/j.geomorph.2022.108236

Huang, F., Tao, S., Chang, Z., Huang, J., Fan, S., Jiang, L., et al. (2021). Efficient and automatic extraction of slope units based on multi-scale segmentation method for landslide assessments. *Landslides* 18, 3715–3731. doi:10.1007/s10346-021-01756-9

Huang, S., He, Y., Yu, S., and Cai, C. (2022a). Experimental investigation and prediction model for UCS loss of unsaturated sandstones under freeze-thaw action. *Int. J. Min. Sci. Technol.* 32, 41–49. doi:10.1016/j.ijmst.2021.10.012

Huang, S., Yu, S., Ye, Y., Ye, Z., and Cheng, A. (2022b). Pore structure change and physico-mechanical properties deterioration of sandstone suffering freeze-thaw actions. *Constr. Build. Mater.* 330, 127200. doi:10.1016/j.conbuildmat.2022.127200

Lai, Y., Hui, H., Ziwang, Z., Songyu, S., and Xuejun, X. (2000). Analytical viscoelastic solution for frost force in cold-region tunnels. *Cold Regions Sci. Technol.* 31, 227–234. doi:10.1016/S0165-232X(00)00017-3

Lai, Y., Liu, S., Wu, Z., and Yu, W. (2002). Approximate analytical solution for temperature fields in cold regions circular tunnels. *Cold Regions Sci. Technol.* 34, 43–49. doi:10.1016/S0165-232X(01)00050-7

Lekhnitskii, S. G. (1981). *Theory of elasticity of an anisotropic body*. Moscow: Mir Publishers.

Li, S., Niu, F., Lai, Y., Pei, W., and Yu, W. (2017). Optimal design of thermal insulation layer of a tunnel in permafrost regions based on coupled heat-water simulation. *Appl. Therm. Eng.* 110, 1264–1273. doi:10.1016/j.applthermaleng.2016.09.033

Li, W., Wu, Y., Fu, H., and Zhang, J. (2015). Long-term continuous *in-situ* monitoring of tunnel lining surface temperature in cold region and its application. *Ijht* 33, 39–44. doi:10.18280/ijht.330206

Li, Y., Sun, Y., Qiu, J., Liu, T., Yang, L., and She, H. (2020). Moisture absorption characteristics and thermal insulation performance of thermal insulation materials for cold region tunnels. *Constr. Build. Mater.* 237, 117765. doi:10.1016/j.conbuildmat.2019.117765

Liu, H., Yuan, X., and Xie, T. (2019). A damage model for frost heaving pressure in circular rock tunnel under freezing-thawing cycles. *Tunn. Undergr. Space Technol.* 83, 401–408. doi:10.1016/j.tust.2018.10.012

Liu, L., Li, Z., Liu, X., and Li, Y. (2018a). Frost front research of a cold-region tunnel considering ventilation based on a physical model test. *Tunn. Undergr. Space Technol.* 77, 261–279. doi:10.1016/j.tust.2018.04.011

Liu, W., Feng, Q., Fu, S., and Wang, C. (2018b). Elasto-plastic solution for cold-regional tunnels considering the compound effect of non-uniform frost heave, supporting strength and supporting time. *Tunn. Undergr. Space Technol.* 82, 293–302. doi:10.1016/j.tust.2018.08.054

Liu, Y., Cai, Y., Huang, S., Guo, Y., and Liu, G. (2020). Effect of water saturation on uniaxial compressive strength and damage degree of clay-bearing sandstone under freeze-thaw. *Bull. Eng. Geol. Environ.* 79, 2021–2036. doi:10.1007/s10064-019-01686-w

Lv, Z., Xia, C., Wang, Y., and Luo, J. (2019). Analytical elasto-plastic solution of frost heaving force in cold region tunnels considering transversely isotropic frost heave of surrounding rock. *Cold Regions Sci. Technol.* 163, 87–97. doi:10.1016/j.coldregions.2019.04.008

Meng, X., Zhang, H., and Liu, X. (2021). Rock damage constitutive model based on the modified logistic equation under freeze–thaw and load conditions. *J. Cold Reg. Eng.* 35, 04021016. doi:10.1061/(ASCE)CR.1943-5495.0000268

Murton, J. B., Ozouf, J.-C., and Peterson, R. (2016). Heave, settlement and fracture of chalk during physical modelling experiments with temperature cycling above and below 0°C. *Geomorphology* 270, 71–87. doi:10.1016/j.geomorph.2016.07.016

Nakamura, D., Goto, T., Ito, Y., Suzuki, T., and Yamashita, S. (2009). "A basic study on frost susceptibility of rock: Differences between frost susceptibility of rock and soil," in *Proceeding of 14th conference on cold regions engineering* (Duluth, Minnesota: ASCE), doi:10.1061/41072(359)11

Nakamura, D., Goto, T., Suzuki, T., Ito, Y., Yamashita, S., Kawaguchi, T., et al. (2012). "Basic study on the frost heave pressure of rocks: Dependence of the location of frost heave on the strength of the rock," in *Cold regions engineering 2012:*

Sustainable infrastructure development in a changing cold environment (Quebec City, Canada: American Society of Civil Engineers), 124–133. doi:10.1061/9780784412473.013

Tan, X., Chen, W., Yang, D., Dai, Y., Wu, G., Yang, J., et al. (2014). Study on the influence of airflow on the temperature of the surrounding rock in a cold region tunnel and its application to insulation layer design. *Appl. Therm. Eng.* 67, 320–334. doi:10.1016/j.applthermaleng.2014.03.016

Xia, C., Lv, Z., Li, Q., Huang, J., and Bai, X. (2018). Transversely isotropic frost heave of saturated rock under unidirectional freezing condition and induced frost heaving force in cold region tunnels. *Cold Regions Sci. Technol.* 152, 48–58. doi:10.1016/j.coldregions.2018.04.011

Yu, H. (2000). *Cavity expansion methods in geomechanics*. Berlin, Heidelberg: Springer Science+Business Media.

Yu, W., Lu, Y., Han, F., Liu, Y., and Zhang, X. (2018). Dynamic process of the thermal regime of a permafrost tunnel on Tibetan Plateau. *Tunn. Undergr. Space Technol.* 71, 159–165. doi:10.1016/j.tust.2017.08.021

Yuanming, Y., Xuefu, X., Wenbing, W., Shujuan, S., Zhiqiang, Z., and Jianzhang, J. (2005). Three-dimensional nonlinear analysis for the coupled problem of the heat transfer of the surrounding rock and the heat convection between the air and the surrounding rock in cold-region tunnel. *Tunn. Undergr. Space Technol.* 20, 323–332. doi:10.1016/j.tust.2004.12.004

Zeng, Y., Liu, K., Zhou, X., and Fan, L. (2017). Tunnel temperature fields analysis under the couple effect of convection-conduction in cold regions. *Appl. Therm. Eng.* 120, 378–392. doi:10.1016/j.applthermaleng.2017.03.143

Zhang, G., Liu, S., Zhao, X., Ye, M., Chen, R., Zhang, H., et al. (2017). The coupling effect of ventilation and groundwater flow on the thermal performance of tunnel lining GHEs. *Appl. Therm. Eng.* 112, 595–605. doi:10.1016/j.applthermaleng.2016.10.120

Zhang, G., Xia, C., Zhao, X., and Zhou, S. (2016). Effect of ventilation on the thermal performance of tunnel lining GHEs. *Appl. Therm. Eng.* 93, 416–424. doi:10.1016/j.applthermaleng.2015.10.008

Zhang, X., Lai, Y., Yu, W., and Zhang, S. (2002). Non-linear analysis for the freezing-thawing situation of the rock surrounding the tunnel in cold regions under the conditions of different construction seasons, initial temperatures and insulations. *Tunn. Undergr. Space Technol.* 17, 315–325. doi:10.1016/S0886-7798(02)00030-5

Zhang, X., Zhou, Z., Li, J., Zhou, Y., and Han, F. (2018). A physical model experiment for investigating into temperature redistribution in surrounding rock of permafrost tunnel. *Cold Regions Sci. Technol.* 151, 47–52. doi:10.1016/j.coldregions.2018.03.007

Zhou, X., Zeng, Y., and Fan, L. (2016). Temperature field analysis of a cold-region railway tunnel considering mechanical and train-induced ventilation effects. *Appl. Therm. Eng.* 100, 114–124. doi:10.1016/j.applthermaleng.2016.01.070